GSA Data Repository item 2018121

“Intracrystalline deformation of calcite in the upper brittle crust”

H. Bauer*, A. Rogowitz, B. Grasemann, K. Decker

*To whom correspondence should be addressed. Email: helene.bauer@univie.ac.at

This file includes text and figures that are divided in to 6 data repository items:

Data Repository Item DR1: Regional geology and local burial and temperature conditions.

Data Repository Item DR2: Tectonic map of the Salzachtal-Ennstal-Mariazell-Puchberg (SEMP) in the investigation area (Styria, Austria).

Data Repository Item DR3: Fault outcrop description.

Data Repository Item DR4: Photos of fault rocks from the Griesgassl Fault.

Data Repository Item DR5: Photos and thin section locations of polished fault rocks from the Griesgassl Fault.

Data Repository Item DR6: Illite Crystallinity

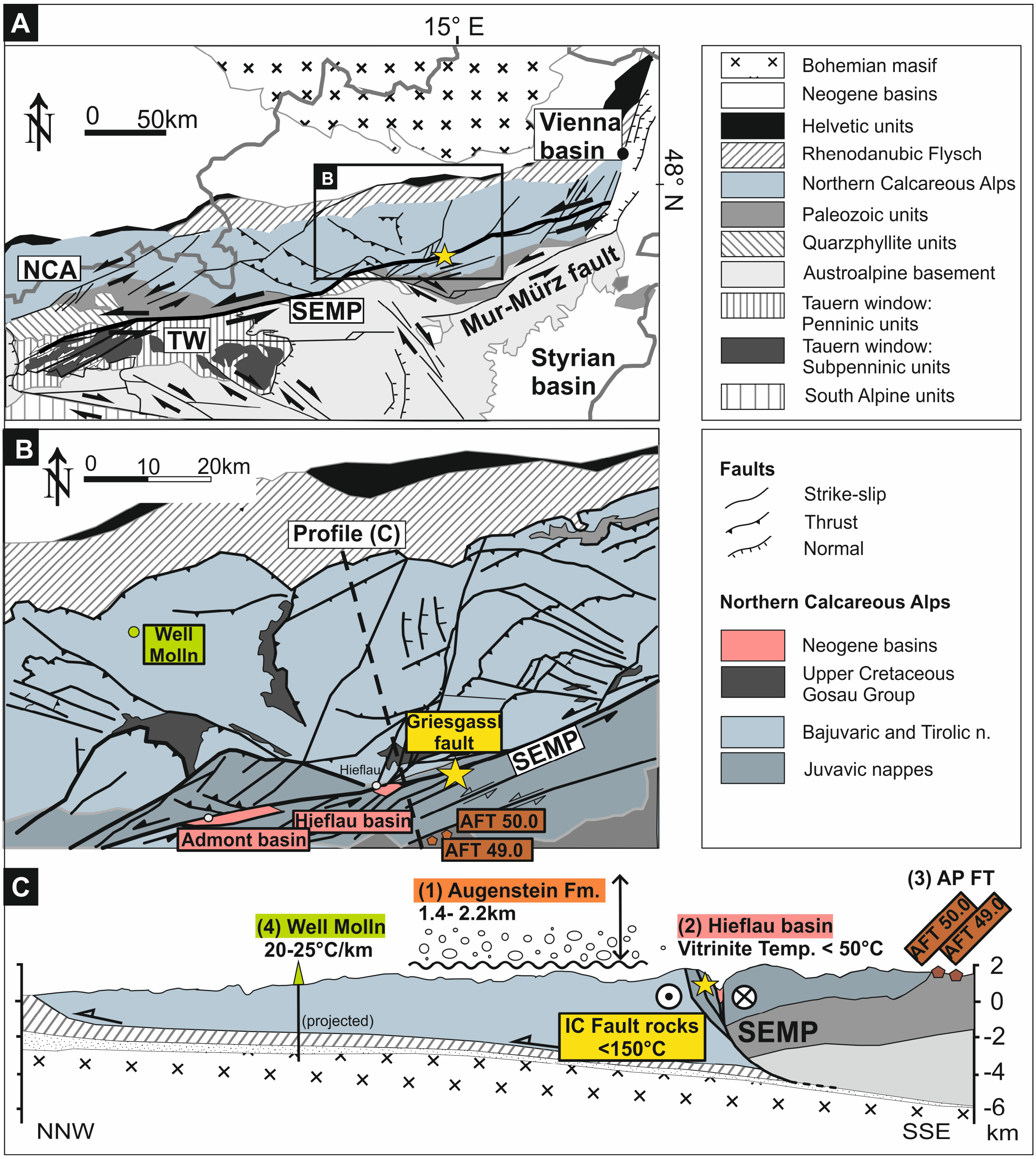

Figure DR1: Regional geology and local burial and temperature conditions.
(A) Tectonic sketch map of the Eastern Alps showing the Salzachtal-Ennstal-Mariazell-Puchberg (SEMP) fault system. Oligocene to Miocene activity of the fault is proved by geochronological data (Urbanek et al., 2002; Glodny et al., 2008) and the ages of fault-bounded sedimentary basins (e.g., Ratschbacher et al., 1991; see Beidinger and Decker, 2014, for a detailed review). The

investigated Griesgassl Fault (marked with yellow star) is a low-displacement splay fault of the SEMP.

(B) Tectonic map of the central segment of the Northern Calcareous Alps showing the SEMP as a broad shear zone with large-scale ENE-striking sinistral faults (after Linzer et al., 2002). Also shown are the locations of the well Molln, Neogene sedimentary basins along the SEMP (Admont, Hieflau) and the sampling points for Apatite fission track data from van Gelder et al (2017). Note the location of the profile shown in C.

(C) Schematic profile through the NCA adopted from Linzer et al. (1995) summarizing regional data that constrain the Oligocene-Miocene burial depth and temperature of the NCA during the formation of the Griesgassl Fault and its fault rocks: (1) Burial of the NCA by the Oligocene-Miocene Augenstein Fm. suggests a burial depth of the sampling point at the Griesgassl fault of < 4 km. The burial depth can be estimated from the thickness of the Augenstein Fm. (1.4 to 2.2 km; Frisch et al., 2001), the observed transgressive contact of the Augenstein Fm. on the Hochschwab Plateau and the elevation of the Griesgassl sampling point about 1.3 km below the plateau (Figure DR2). (2) Vitrinite reflection data from the Neogene basins along the SEMP fault indicate very low thermal overprint (R<0.7%; Sachsenhofer, 1992) and burial temperatures below 100° (calculated after Barker and Pawlewicz, 1994). (3) Apatite fission track cooling ages of about 50 Ma (van Gelder, 2017) from the Paleozoic units (Noric nappe) below the NCA show that these units cooled below about 100°C during the Eocene, i.e., before the onset of faulting of the SEMP. (4) Projection of the well Molln drilling through the NCA. The current geothermal gradient measured in the 5 km deep borehole is about 20-25°C/km.

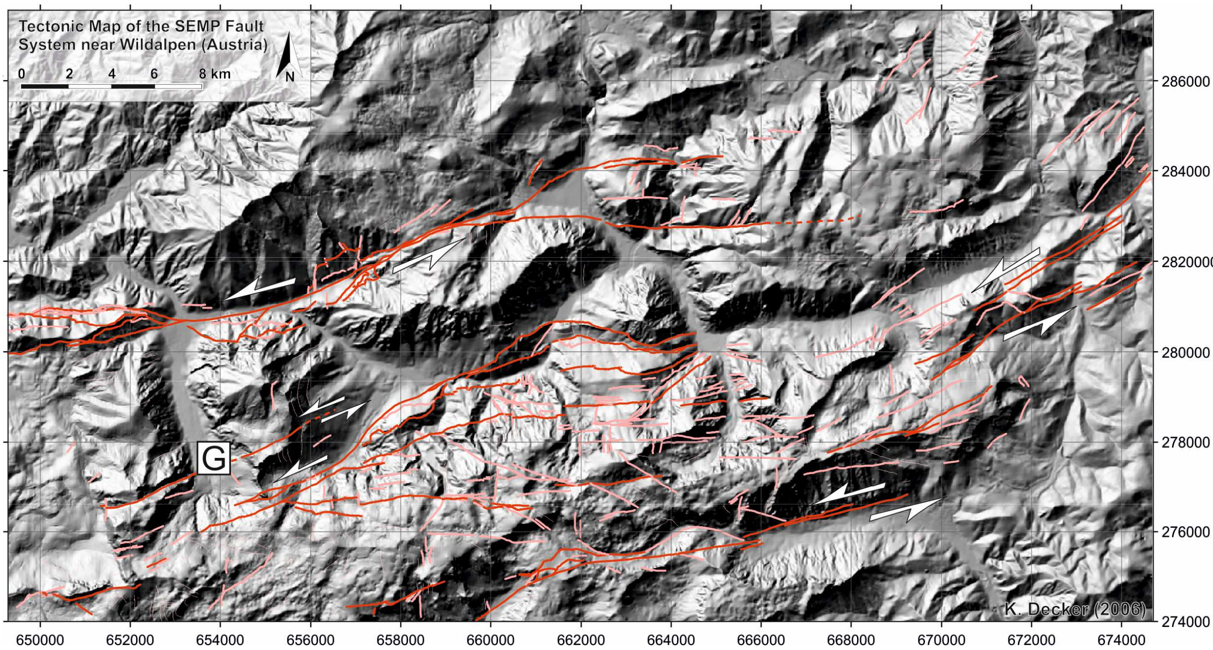

Figure DR2: Tectonic map of the Salzachtal-Ennstal-Mariazell-Puchberg (SEMP) in the investigation area (Styria, Austria). See Fig. 1 in the main text for location. The fault forms an up to 15 km broad shear zone composed of anastomosing WSW-ENE-striking and W-E-striking sinistral strike-slip faults with flower structures and convergent strike-slip duplexes. The investigated fault (referred to as Griesgassl Fault, marked with G) is a splay fault of the SEMP accommodating an estimated maximum offset of few hundred meters. Coordinates refer to the Austrian Grid GKM M 34.

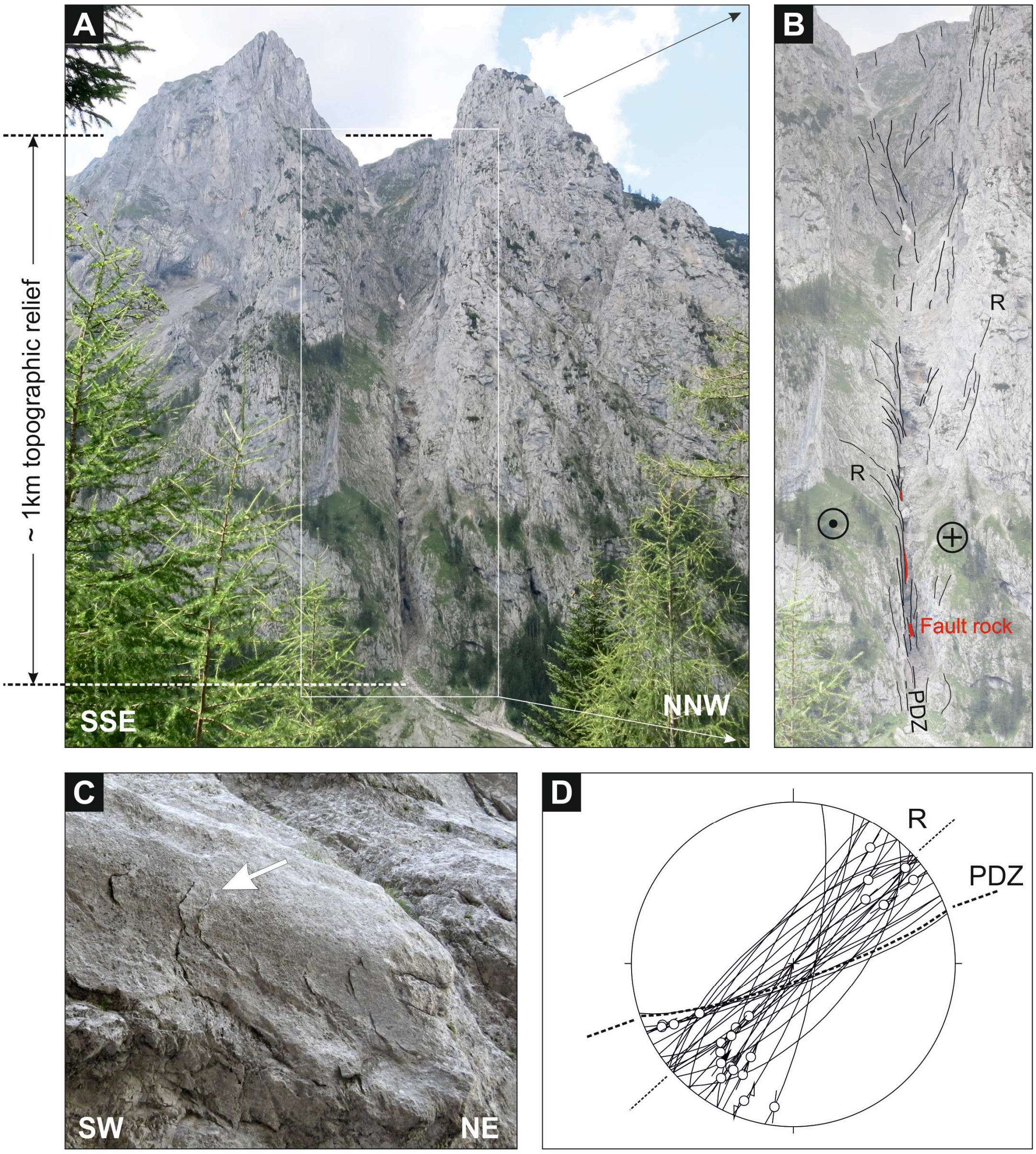

Figure DR3: Fault outcrop description. **(A)** Panoramic view of the Griesgassl Fault (outcrop coordinates: 277.300 E, 653.400 W, Austrian Grid GKM M 34; Lat 47.62717 Long 15.04682) view towards W. The fault is exposed over a topographic relief of about 1 km. **(B)** Enlarged detail from (A) highlighting faults that were mapped in accessible outcrops at the base of the section and along the crest on top. Note the narrow principle displacement zone (PDZ) with fault rock (highlighted in red) exposed. The convex-up faults branching from the PDZ are synthetic Riedel shears (R). **(C)** Fault plane of a synthetic Riedel shear with sub-horizontal striation and lunate fractures (arrow) proofing sinistral strike-slip displacement. **(D)** Fault slip data from the outcrop at the base of the cliff. The orientation of the PDZ his highlighted. Most of the recorded faults are synthetic Riedel shears (R).

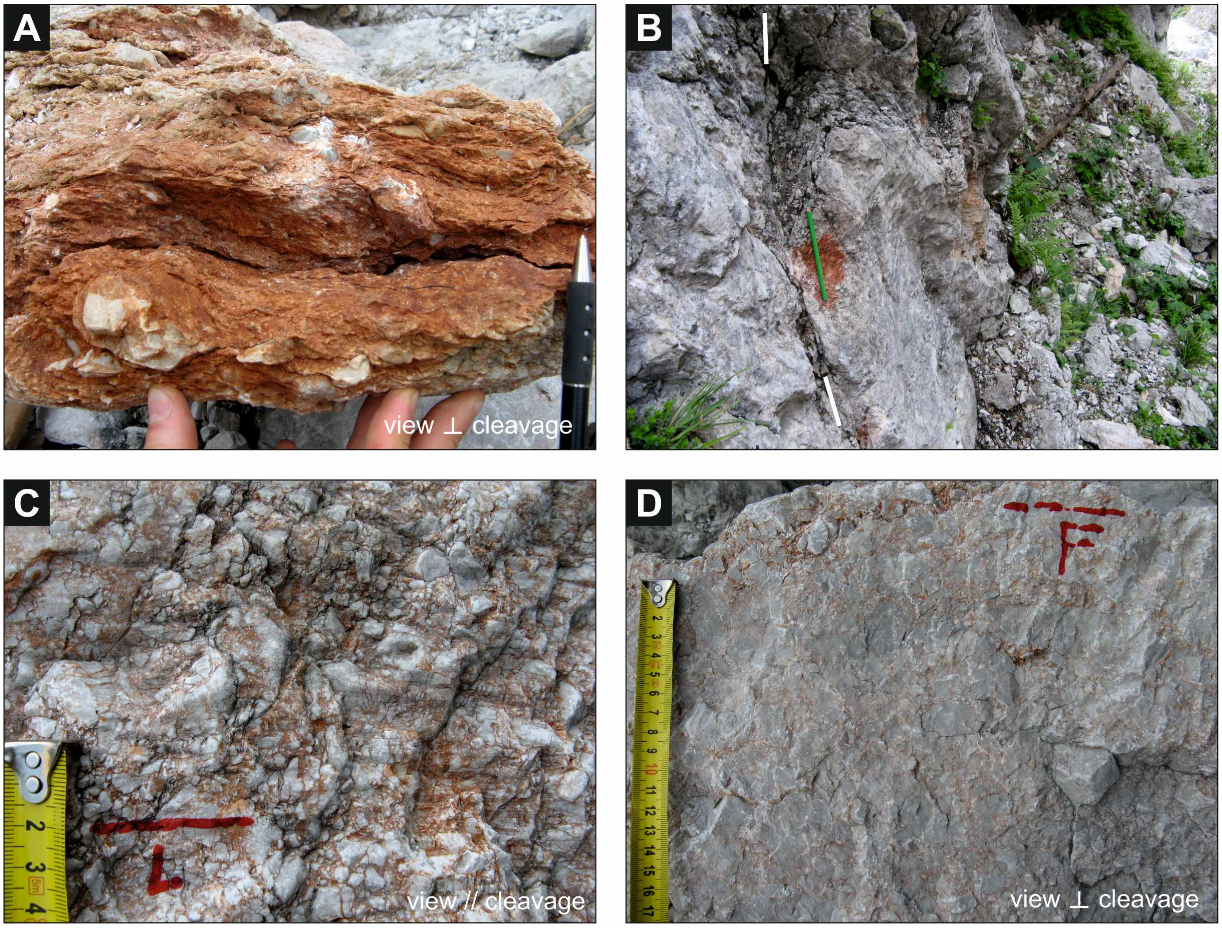

Figure DR4: Photos of fault rock from the Griesgassl Fault. **(A)** Specimen of one of the foliated clay-supported fault rocks analyzed in this paper. **(B)** Red foliated clay-rich fault rock comprised between fault planes of a synthetic Riedel shear. Outcrop about 20 m south of the PDZ at the base of the cliff shown in Figure 2. (C) (D) Structures in fault rock observed from fallen blocks. **(C)** Striated fault rock with limestone fragments and stylolites seen on a plane parallel to foliation. L indicates the direction of the lineation. **(D)** Anastomosing stylolites seen on a rock surface perpendicular to the foliation, but oblique to the slip direction of the fault rock. Note the preferred orientation of stylolites parallel to the foliation of the fault rock. F indicates the direction of foliation.

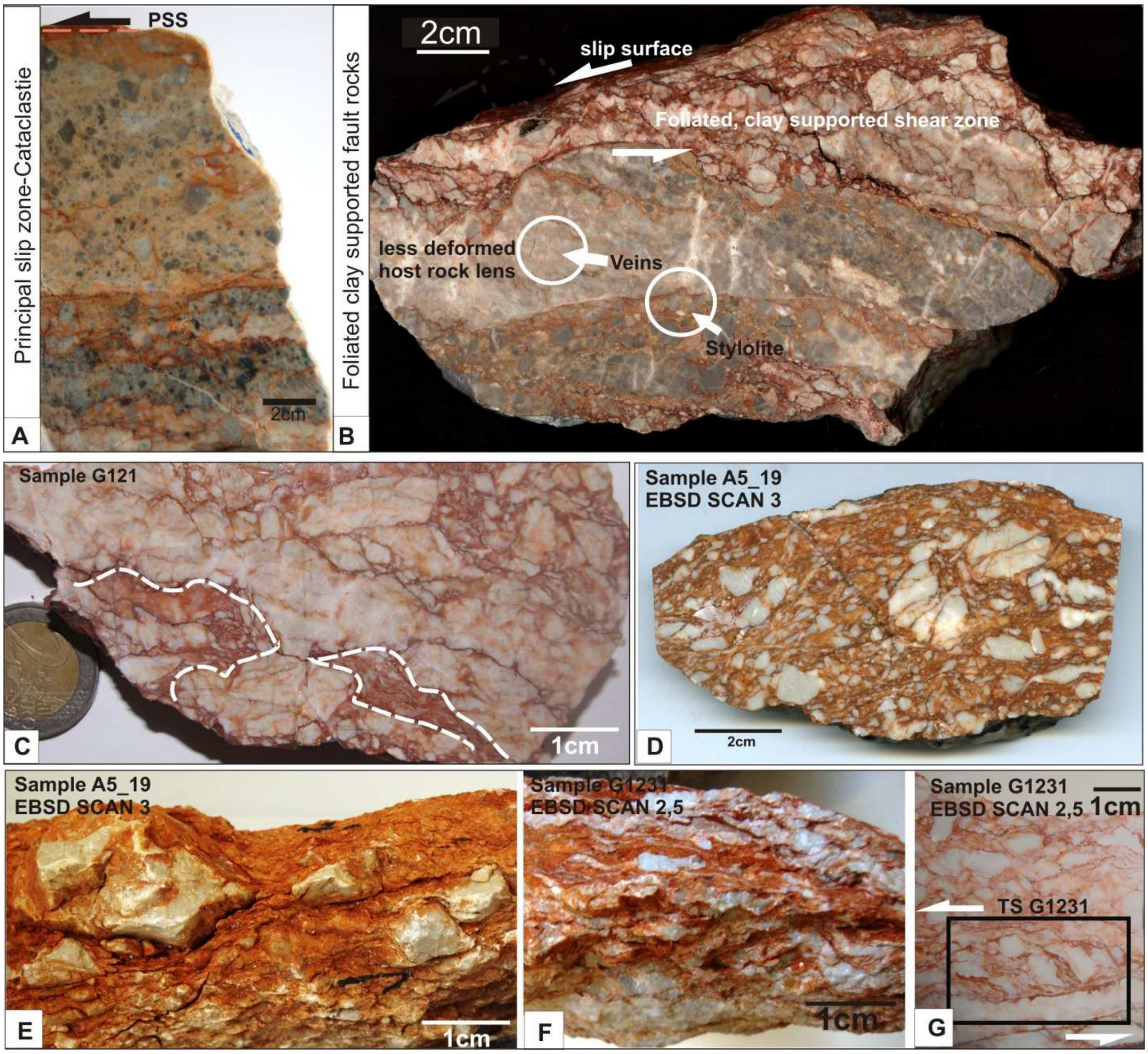

Figure DR5: Photos of polished fault rock from the Griesgassl Fault. **(A)** Cut and polished hand specimens of cataclasite fault rock forming the Principal Slip Zone of the fault. Note: Stylolites formed along cataclastic fault rocks. **(B)** Foliated clay supported fault rock taken from the locality shown in Figure DR3 (B). **(C)** Less foliated, dissolution dominated fault rock lacking evidence for MSZs. **(D)**, **(E)** Strongly foliated fault rock with > 1cm sized microlithons, from which EBSd scan 3 was done. **(F)** Strongly foliated fault rock with elongated microlithons exclusively < 1cm. **(G)** Thin section location from which EBSD scans 3 and 5 were done is marked with the black frame.

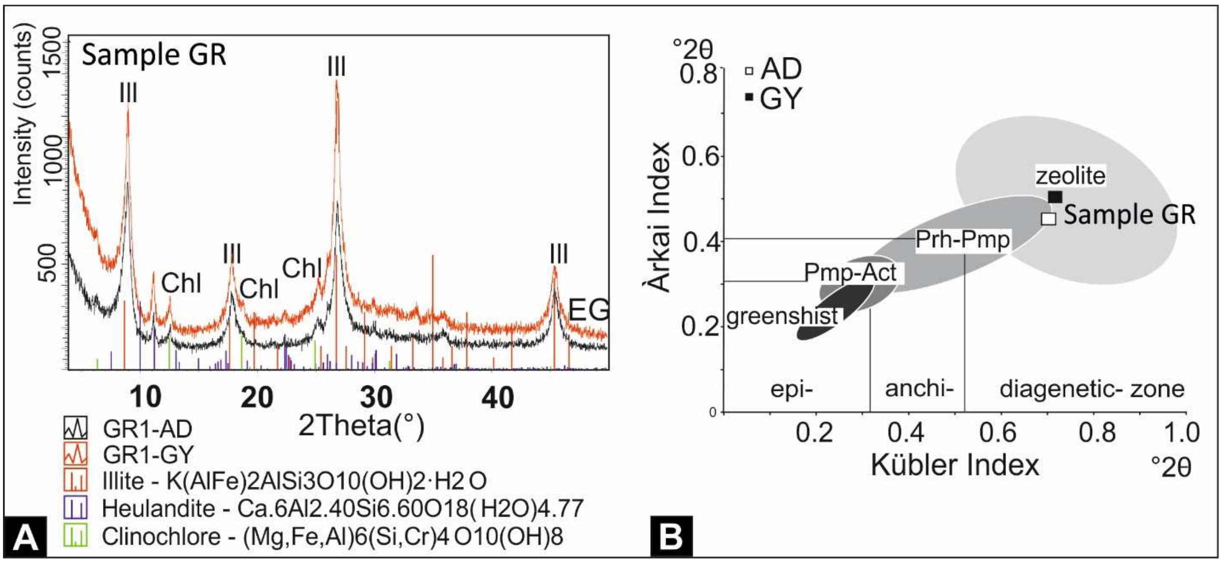

Figure DR6: (A) The fine grained matrix in clay residues in MCC fault rocks is made of illite and chlorite. In the presented sample we additionally found heulandite, a zeolite mineral. Illite crystallinity from our sample was calculated using the XRD graph shown in A. **(B)** Plotting Kübler against Arkai Index reveals zeolite facies burial conditions for the clays. In accordance with the observation of heulandite this would place the illites in a digenetic zone with a temperature of around 100-150° C.

References

Barker, C.E. and Pawlewicz, M. J., 1994, Calculation of vitrinite reflectance from thermal histories and peak temperatures: a comparison of methods, *in* Mukhopadhyay, P.K. and Dow, W.G., eds., Re-evaluation of Vitrinite Reflectance as a Rank Parameter, American Chemical Society Symposium Series, chapter 14, p. 216-229.

Beidinger, A. and Decker, K., 2014, Quantifying Early Miocene in-sequence and out-of-sequence thrusting at the Alpine-Carpathian junction, Tectonics, v. 33, p. 222-252.

Frisch, W., Kuhlemann, J., Dunkl, I. and Székely, B., 2001, The Dachstein paleosurface and the Augenstein Formation in the Northern Calcareous Alps – a mosaic stone in the geomorphological evolution of the Eastern Alps, International Journal of Earth Sciences, v. 90, p. 500-518.

Glodny, J., Ring, U. and Kühn, A., 2008, Coeval high-pressure metamorphism, thrusting, strike-slip and extensional shearing in the Tauern Window, Eastern Alps, Tectonics, v. 27, p. 27.

Linzer, H.G., Ratschbacher, L. and Frisch, W., 1995, Transpressional collision structures in the upper crust: the fold-thrust belt of the Northern Calcareous Alps, Tectonophysics, v.242, p.41-61.

Linzer, H.G., Decker, K., Peresson, H., Dell`Mour, R. and Frisch, W., 2002, Balancing lateral orogenic float of the Eastern Alps: Tectnonophysics, v. 354, p. 211–237.

Ratschbacher, L., Frisch, W. and Linzer, H. G., 1991, Lateral extrusion in the eastern Alps, part II: Structural analysis, Tectonics, v. 10(2), p. 257–271.

Sachsenhofer, R., 1992, Coalification and thermal history of Tertiary basins in relation to late Alpidic evolution of the Eastern Alps. Geol. Rundschau, v. 81, p. 291-308.

Urbanek, C., W. Frank, B. Grasemann and K. Decker, 2002, Eoalpine versus tertiary deformation: Dating of heterogeneously partitioned strain (Tauern Window, Austria), paper presented at PANGEO Austria 2002, Salzburg. [Available at http://web400.login-3.hoststar.at/www.christoph_urbanek.at/ images/POSTER.PANGEO.SEMP.2002.pdf.]

Van Gelder, I, 2017, Interfering orogenic processes derived from Alps-Adria interactions [Ph.D.thesis], Utrecht, University of Utrecht, 172 p.